

**Title:**

Novel Oral Derivative UD-017, a Highly Selective CDK7 Inhibitor, Exhibits Anticancer Activity by  
Inducing Cell-Cycle Arrest and Apoptosis in Human Colorectal Cancer

**Authors' full names:**

Yasuhiro AGA<sup>1,2,\*</sup>, Takashi MATSUSHITA<sup>2</sup>, Sayaka OGI<sup>2</sup>, Kazuhiro ONUMA<sup>2</sup>, Hidetoshi  
SUNAMOTO<sup>2</sup>, Ayumi OGAWA<sup>2</sup>, Shigeyuki KONO<sup>2</sup>, Noriaki IWASE<sup>2</sup>, Yasunori TOKUNAGA<sup>2</sup>,  
Shigeru USHIYAMA<sup>2</sup>, Futoshi NARA<sup>2</sup>, Yasushi KONNO<sup>2</sup>, Masao YOSHIZUMI<sup>1</sup>, Hiroki  
KOKUBO<sup>1</sup> and Kenji YONEDA<sup>2</sup>

1) Department of Cardiovascular Physiology and Medicine, Graduate School of Biomedical &  
Health Sciences, Hiroshima University, Japan

2) Pharmaceuticals Research Laboratory, Pharmaceutical Division, Chemicals Company, UBE  
Industries, Ltd., 1978-5, Kogushi Ube, Yamaguchi, Japan

\*) Corresponding author: Yasuhiro AGA.

Pharmaceuticals Research Laboratory, Pharmaceutical Division, Chemicals Company, UBE  
Industries, Ltd., 1978-5, Kogushi Ube, Yamaguchi, Japan

Tel: +81-836-31-6405, E-mail: 30205u@ube-ind.co.jp

**Running title:** Anticancer Effect of UD-017

**Key words:** UD-017, CDK7 inhibitor, colorectal cancer, HCT-116

## ABSTRACT

**Objective:** This study aimed to investigate the anticancer profile of a new cyclin-dependent kinase 7 (CDK7) inhibitor, UD-017, by examining its mechanism of action using HCT-116 colorectal cancer cells.

**Methods:** The anticancer properties of UD-017 were assessed using several assays, including *in vitro* kinase, proliferation, and apoptosis assays, western blot analysis, and an *in vivo* xenograft mouse model.

**Results:** UD-017 significantly inhibited CDK7 activity ( $IC_{50} = 16$  nM) with high selectivity in an *in vitro* kinase assay testing a panel of over 300 proteins and lipid kinases. UD-017 also inhibited the growth of HCT-116 cells ( $GI_{50} = 19$  nM) and inhibited the phosphorylation of various downstream mediators of CDK7 signaling. In cell cycle and apoptosis assays using HCT-116 cells, UD-017 increased the number of cells in both G1 and G2/M phases and induced apoptosis. *In vivo*, UD-017 inhibited tumor growth in an HCT-116 xenograft mouse model by 33%, 64%, and 88% at doses of 25, 50, and 100 mg/kg, respectively, with clear dose-dependency. Co-administration of 5-FU and 50 mg/kg UD-017 had a strong synergistic effect, as reflected in the complete inhibition of tumor growth.

**Conclusion:** CDK7 may play a major role in colorectal cancer growth by regulating the cell cycle and apoptosis. UD-017 is a promising candidate therapeutic agent for the treatment of cancer involving CDK7 signaling.

## INTRODUCTION

Cyclin-dependent kinases (CDK) are serine/threonine kinases that regulate multiple cellular processes<sup>19</sup>. CDK7 was identified as a component of CDK-activating kinase (CAK), which plays a pivotal role in cell cycle progression<sup>10</sup>. CAK phosphorylates threonine residues in the activation segment (T-loop) of downstream CDKs, including *cdc-2*/CDK1, CDK2, CDK4, and CDK6, and modulates their activities<sup>25</sup>. CDK7 plays another important role in transcription via phosphorylation of the carboxyl-terminal domain (CTD) of RNA polymerase II (RNAPII)<sup>1,5,11,16</sup>. Specifically, the general transcription factor II (TFIIH) complex (containing CDK7 and cyclin H) phosphorylates serine-5 of the CTD, thereby enhancing the association between the CTD and m7G RNA capping machinery<sup>1</sup>. TFIIH also phosphorylates the serine-7 residue of the CTD and modulates pausing and transcriptional termination<sup>5,11</sup>.

The super-enhancer, first proposed by Young et al.<sup>12</sup> is a huge cluster of enhancers and formed by transcription factors and co-factors. The expression of several oncogenes, including *Myc*, is regulated by super-enhancers<sup>18,20</sup>. The inhibition of CDK7 downregulates super-enhancer-mediated gene expression in cancer cells, including the expression of *Myc* and other oncogenes<sup>7</sup>.

To date, several CDK inhibitors (including the pan-CDK inhibitor Flavopiridol) have been tested in clinical trials and found to be highly toxic<sup>30</sup>. However, a number of selective CDK4/6 inhibitors (e.g., Palbociclib, Ribociclib, and Abemaciclib) have been approved for the treatment of breast cancer, with

ongoing trials with other types of cancer<sup>3,9,26</sup>). This suggests that the selective inhibition of CDKs could be the key to reducing the cytotoxicity observed with some CDK inhibitors.

CDK7 expression correlates with malignancy in many cancers, such as gastric cancer<sup>28</sup>), esophageal squamous cell carcinoma<sup>31</sup>), breast cancer<sup>23</sup>), and colorectal cancer<sup>34</sup>), suggesting that CDK7 is an attractive target for cancer therapy. The present study aimed to evaluate the pharmacodynamic properties and anticancer activity of the highly selective, orally bio-available CDK7 inhibitor, UD-017, in the context of colorectal cancer.

## **MATERIALS AND METHODS**

### **Animals**

Five-week-old female athymic BALB/c<sup>nu/nu</sup> nude mice (CAnN.Cg-Foxn1<sup>tm1.1</sup>/Crj) were obtained from Charles River Laboratories Japan, Inc. (Kanagawa, Japan). All animals were acclimatized to the laboratory environment for about one week and were confirmed to be healthy prior to use in experiments. The mice were housed in barrier facilities and kept under controlled environmental conditions at a room temperature of  $23 \pm 2^\circ\text{C}$  and  $55 \pm 10\%$  humidity on a 12-hr light/dark cycle with ventilation (15 air changes/hr). The mice were fed with a regular  $\gamma$ -ray-sterilized chow diet and 0.5  $\mu\text{m}$  filtered water *ad libitum* via water bottles (which were replaced twice a week). All experimental protocols were reviewed and approved by the Animal Care and Use Committee of the Pharmaceuticals Research Laboratory of Ube Industries Ltd.

### **Compound**

UD-017 was synthesized at the Drug Research Institute, Research and Development Division, Ube Industries Ltd. (described in International Patent Publication WO2016/204153A1). 5-Fluorouracil (5-FU) was purchased from Wako Pure Chemical Industries, Ltd. (Osaka, Japan).

### **Kinase panel assay**

The ability of UD-017 (1000 nM) to inhibit kinases was tested against a panel of 313 kinases by either an off-chip mobility shift assay or IMAP assay (Molecular Devices LLC., Sunnyvale, USA).

For AMPK $\alpha$ 2/ $\beta$ 1/ $\gamma$ 1, AMPK $\alpha$ 1/ $\beta$ 1/ $\gamma$ 1, GSK3 $\beta$ , and CDKs, additional inhibition tests were conducted by optimal range of concentrations to decide the concentration of UD-017 required to suppress each enzyme by 50% (IC<sub>50</sub>). These assays were performed by Carna Biosciences, Inc. (Kobe, Japan). IC<sub>50</sub> was calculated using the EXSUS (Version 8.1; CAC Croit Corporation. Tokyo, Japan) statistical analysis system.

#### **Cell proliferation assay (cancer cell line panel)**

All cell lines were obtained from the American Type Culture Collection (ATCC, Manassas VA, USA). An assay stock was thawed and diluted in ATCC-recommended medium and was dispensed in a 384-well plate. Plated cells were incubated in 5% CO<sub>2</sub> at 37°C. After 24 hrs, diluted UD-017 was added, and the plates were further incubated for another 72 hrs. After incubation, the cells were counted according to ATP quantity, and GI<sub>50</sub> values (concentrations that produced 50% growth inhibition) were calculated from the dose-response sigmoidal curve. These cell proliferation assays were performed using Oncolines™ (Netherlands Translational Research Center B.V., Oss, Netherlands).

#### **Cell culture (HCT-116 cells)**

HCT-116 cells (colorectal cancer cell line) were obtained from DS Pharma BioMedical (EC91091005-F0) and cultured in McCoy's 5A medium (16600-082, GIBCO) supplemented with 10% fetal bovine serum (11082, GIBCO) and 1% antibiotic–antimycotic solution (15240-096, GIBCO). Cells were incubated in a humidified atmosphere of 5% CO<sub>2</sub> at 37°C.

### **Western blot analysis (*in vitro* experiments)**

HCT-116 cells were lysed in RIPA buffer (9806S, Cell Signaling Technology, Danvers, USA) or M-PER (78510, Thermo Fisher Scientific, Inc., Waltham, USA) that contained both protease inhibitors (Complete Mini, Roche Diagnostics, Mannheim, Germany) and phosphatase inhibitors (Complete PhosSTOP, Roche Diagnostics, Mannheim, Germany). Cell lysates were subjected to SDS-PAGE and western blot analysis. Immunoblots were probed with primary antibodies and subsequently with their respective horseradish peroxidase–conjugated secondary antibodies. The primary antibodies used were as follows: anti-GAPDH antibody (2118S), anti-Rb antibody (9309S), anti-phospho-Rb S780 antibody (8180S), anti-phospho-Rb S807/811 antibody (8516S), anti-cdc2 antibody (9112S), anti-phospho-cdc2 Thr161 antibody (9116S), anti-CDK2 antibody (2546S), anti-phospho-CDK2 Thr160 (2561S), anti-c-Myc antibody (5605S), anti-PARP antibody (9542), and anti-XIAP antibody (2042), all of which were purchased from Cell Signaling Technology, Inc. The anti-phospho-Rb S795 antibody (ab47474) and anti-RNAPII antibody (ab817) were purchased from Abcam, and the anti-RNAPII CTD P-ser2 antibody (04-1571), anti-RNAPII CTD P-ser5 antibody (04-1572), and anti-RNAPII CTD P-ser7 antibody (04-1570) were purchased from Merck Millipore Corporation. Immunoblots were developed with the Amersham™ ECL™ Prime Western Blotting Detection Reagent (GE Healthcare, Buckinghamshire, UK), and chemiluminescence was captured with a ChemiDoc™ XRS System (Bio-Rad Laboratories, Inc., Hercules, USA).

### **Cell cycle assay**

HCT-116 cells were seeded in six-well plates and allowed to adhere overnight. DMSO or UD-017 was added to the cells for 8 hrs, after which cells were collected and treated in accordance with the manufacturer's protocol (Cell-Cycle Phase Determination Kit, 10009349, Cayman Chemical Company, Ann Arbor, USA). A minimum of 10,000 events were collected per sample for flow cytometry analysis (FACSCalibur, Becton Dickinson, Franklin Lakes, USA). Cell cycle analysis was performed using ModFit LT software (Verity Software House, Topsham, USA). Data are presented as mean values (n = 2).

### **Apoptosis assay**

HCT-116 cells were seeded onto plates overnight. The following day, UD-017 was added to each well at final concentrations of 100, 300, 1000, 3000, and 10,000 nM, and DMSO was added as a control (final DMSO concentration: 0.1%). The cells were then incubated for 72 hrs. The culture medium was removed after incubation and the cells were collected. FITC Annexin V and propidium iodide (PI) were added to the cells (FITC Annexin V apoptosis detection kit I, 556547, BD Pharmingen, San Jose, USA). After incubation, the cells were analyzed within 1 hr by flow cytometry. Data are presented as mean values  $\pm$  SD (n = 3–6).

### **Xenograft mouse model**

HCT-116 cells were harvested and diluted in phosphate-buffered saline to produce a cell suspension

of  $1 \times 10^7$  cells/100  $\mu$ l. The cell suspensions (100  $\mu$ l/mouse) were injected into the right flanks of mice. At 6–7 days after injection, tumor volume ( $\text{mm}^3$ ) was calculated as follows:  $([\text{Ma}] \times [\text{Mi}] \times [\text{Mi}])/2$  (where Ma is the length of the major axis, and Mi is the length of the minor axis). Once tumors reached a size of about 100  $\text{mm}^3$ , the mice were selected and grouped so that the mean tumor volumes of all groups ( $n = 6$ ) were approximately equal. UD-017 was suspended in 0.5% (w/v) methyl cellulose 400 solution and orally administered daily from day 0 to day 13 for two weeks. 5-fluorouracil (5-FU) was dissolved in a glucose injection solution (20%, Otsuka Pharmaceutical Co. Ltd., Tokyo, Japan) and intraperitoneally administered at a dose of 15 mg/kg daily for two weeks. During the experiments, mice were weighed and tumors were measured twice weekly. Data are presented as mean values  $\pm$  SEM ( $n = 6$ ).

#### **Western blot analysis (*in vivo*)**

Fourteen days after HCT-116 cell injection, mice were orally administered 25, 50, or 100 mg/kg of UD-017 or vehicle. Two hours after administration of a single dose, tumors were collected under isoflurane anesthesia. T-PER (78510, Thermo Fisher Scientific Inc.) and a Halt protease and phosphatase inhibitor cocktail (100 $\times$ ) were mixed at a ratio of 100:1 to prepare the lysis buffer. Protein lysates from tumors were subjected to SDS-PAGE and Western blot analysis. Immunoblots were probed with primary antibodies (anti-GAPDH antibody [2118S], anti-c-Myc antibody [5605S], anti-Rb [4H1], anti-phospho-Rb [Ser780] [D59B7], and anti-PARP antibody [9542S] from Cell Signaling

Technology Inc.; anti-RNA pol2 antibody [ab817] from Abcam; and anti-RNA pol2 CTD P-ser5 antibody [04-1572] from Merck Millipore Corporation), followed by their respective horseradish peroxidase-conjugated secondary antibodies. Immunoblots were developed using the Amersham™ ECL™ Prime Western Blotting Detection Reagent (GE Healthcare) and chemiluminescence was captured with a ChemiDoc™ XRS System (Bio-Rad Laboratories).

### **Densitometry**

Analysis of the bands on films was performed using Image Lab (Molecular Imager® ChemiDoc™ XRS). The target band was identified based on molecular weights of both the target protein and the detected band. Using this software, band densities were quantified at an appropriate interval and output.

### **Statistical analysis**

Statistical analyses were performed with EXSUS software using analysis of variance followed by Dunnett's multiple test. P-values less than 0.05 were considered significant.

## **RESULTS**

### **Kinase selectivity of UD-017**

The kinase selectivity of UD-017 was tested using the off-chip mobility shift assay or IMAP assay.

UD-017 at 1000 nM was highly selective for CDK7 among the 313 kinases tested (Figure 1A). Only four kinases (AMPK $\alpha$ 2/ $\beta$ 1/ $\gamma$ 1, AMPK $\alpha$ 1/ $\beta$ 1/ $\gamma$ 1, GSK3 $\beta$ , and Haspin) were inhibited by more than 50% at UD-017 concentrations <1000 nM, but the IC<sub>50</sub> values for these kinases were still  $\geq$ 20-fold higher than that for CDK7. Selectivity among CDK subtypes was also confirmed. IC<sub>50</sub> values for CDK7 were  $\geq$ 300-fold higher than for other CDKs, including CDK1, CDK2, CDK3, CDK4, CDK5, CDK6, and CDK9 (Figure 1B).

### **Antiproliferative activity of UD-017**

The antiproliferative effect of UD-017 was initially tested against a panel of cancer cell lines (Oncolines™). UD-017 showed significant growth inhibition with a GI<sub>50</sub> of 19 nM for HCT-116 cells (Figure 1C). We next looked into the mechanism underlying the antiproliferative activity of UD-017. CDK7 is a member of the cyclin-dependent kinase family and regulates the activities of other CDKs (such as CDK1, CDK2, and CDK4/6) by phosphorylating their activation segments. The phosphorylation of retinoblastoma (Rb) by CDK2 or CDK4/6 controls the cell cycle. Therefore, we tested the effect of UD-017 on the phosphorylation of CDKs and Rb in HCT-116 cells. Treating HCT-116 cells with 100 and 1000 nM of UD-017 for 8 hrs and 24 hrs reduced CDK-1 and CDK-2 phosphorylation. The suppression of Rb phosphorylation at CDK4/6-specific sites (Ser780 and Ser807/811)<sup>32</sup> suggests that UD-017 inhibited the activities of CDK4/6 (Figure 2A). Cell cycle analyses revealed that HCT-116 cells treated with 100 nM and 1,000 nM of UD-017 for 8 hrs increased

the number of cells in both G<sub>1</sub> and G<sub>2</sub>/M phases (Figure 2B).

### **Effects of UD-017 on transcriptional machinery and oncogene expression**

CDK7 phosphorylates serine in the CTD of RNAPII and controls transcriptional initiation and elongation by RNAPII<sup>1,5,11,16</sup>). In this experiment, we examined the effects of UD-017 on RNAPII phosphorylation in HCT-116 cells. As shown in Figure 3A, UD-017 potently inhibited serine 5 phosphorylation of RNAPII for up to 72 hrs after treatment, but did not inhibit serine 7 phosphorylation.

Given reports that transcriptional inhibition by CDK7 has a large effect on the expression of oncogenes such as Myc<sup>7</sup>), we also examined c-Myc expression. c-Myc expression was inhibited by UD-017 at 100 and 1000 nM in HCT-116 cells (Figure 3B). This suggests that suppression of transcription through the inhibition of RNAPII phosphorylation by UD-017 might lead to a sustained inhibition of c-Myc expression.

### **Effects of UD-017 on apoptosis**

The expression of apoptotic signaling proteins in HCT-116 cells at 72 hrs after treatment with UD-017 was examined. At concentrations  $\geq 100$  nM, the expression of XIAP, an anti-apoptotic molecule, decreased, and PARP cleavage increased in a dose-dependent manner (Figure 3C). Given the activation of apoptotic signaling, the proportion of Annexin V-positive and PI-negative cells (which reflect early apoptotic cells) was investigated using flow cytometry. As shown in Figure 3D, UD-017

induced apoptosis from a concentration of 100 nM, with the increase becoming significant at concentrations above 1000 nM.

### **Anticancer effect of UD-017 *in vivo***

Since UD-017 exhibited antiproliferative effects *in vitro*, we next tested whether UD-017 has anticancer effects *in vivo* using an HCT-116 xenograft mouse model. Daily single doses of UD-017 at 25, 50, and 100 mg/kg inhibited cancer growth by 33%, 64%, and 88%, respectively, with clear dose-dependency over the course of 14 days (Figure 4A). Throughout the experiment, UD-017 was well tolerated, with no reduction in body weight (Figure 4B).

To gain a better understanding of the mechanism underlying the anticancer effect of UD-017 after single dosing, the expression levels of various proteins in tumors were assessed at 2 hrs after UD-017 administration. Similar to the *in vitro* experiments, phosphorylation of Rb at S780 was inhibited, reflecting cell cycle arrest (Figure 5A). UD-017 also inhibited RNAPII phosphorylation and c-Myc expression starting at a dose of 25 mg/kg. PARP cleavage was detected from 50 mg/kg (Figure 5B). These findings suggest that UD-017 induces apoptosis both *in vitro* and *in vivo*.

### **Combination therapy with UD-017 and 5-FU**

Since 5-FU is the standard drug used for chemotherapy in colorectal cancer, we tested the combined effect of UD-017 with 5-FU. Tumor-bearing mice were treated with 15 mg/kg i.p. of 5-FU alone, 50 mg/kg of UD-017 alone, or UD-017 plus 5-FU. As shown in Figures 6A and 6B, an additive effect on

the reduction of tumor volume was observed with the combination of UD-017 with 5-FU, with no side effects.

## **DISCUSSION**

This is the first report of the anticancer effects of UD-017, a newly identified, orally bio-available, potent, and selective CDK7 inhibitor. UD-017 has been shown to exhibit anticancer effects by inducing cell cycle arrest and apoptosis. Several CDK7 inhibitors have been shown to have marked anticancer effects in preclinical studies<sup>2,8,13,17,27,33</sup>). There is also a currently ongoing trial of CT7001, another orally bio-available selective CDK7 inhibitor, for breast cancer<sup>24</sup>).

Testing the inhibitory activity of UD-017 against a panel of 313 kinases revealed that UD-017 showed minimal inhibition of kinases other than CDK7, demonstrating its high specificity for CDK7. This supports the low risk of UD-017 in terms of inducing unexpected adverse reactions resulting from the inhibition of other kinases<sup>4</sup>). Unlike THZ1 (which covalently binds to CDK7<sup>8</sup>), the inhibition of CDK7 by UD-017 is reversible (data not shown). Thus, UD-017 has a very favorable profile with regard to efficacy and toxicity.

UD-017 was found to inhibit the phosphorylation of CDK1, CDK2, and Rb (Ser780, Ser795, and Ser807/811), and slightly increased the proportion of cells in G<sub>1</sub> and G<sub>2</sub>/M phases. The modest effect on arrest at specific cell cycle phases could reflect the fact that UD-017 caused cell cycle arrest as a

whole, rather than at a particular phase. According to recent studies, some cancers have acquired resistance to CDK4/6 inhibitors<sup>22</sup>). Since the role of CDK7 is not limited to the G1 phase of the cell cycle, CDK7 inhibitors may be effective against cancers resistant to CDK4/6 inhibitors. In addition to its effect on the cell cycle, UD-017 suppressed transcription by inhibiting the phosphorylation of RNAPII, regulated the expression of an apoptosis-related protein (XIAP), and induced apoptosis. These findings collectively suggest that UD-017 selectively inhibits CDK7 and exerts an anticancer effect by arresting the cell cycle and inducing apoptosis both *in vitro* and *in vivo*. This mechanism of action has also been reported for other CDK7 inhibitors<sup>13,15,24</sup>).

Myc inhibition is an attractive target for cancer treatment. However, directly inhibiting Myc is difficult because it structurally lacks a pocket for modulators and has a short life<sup>29</sup>). One practical approach to inhibiting Myc is to regulate its expression<sup>29</sup>). For example, small-molecule ligands targeting c-Myc promoter G-quadruplexes and small-molecule inhibitors of c-Myc/Max/DNA complex formation have been reported<sup>6</sup>). CDK7 regulates the super-enhancer-driven transcription of Myc and other oncogenes<sup>7</sup>). In the present study, we demonstrated that UD-017 inhibits the phosphorylation of RNAPII, suppresses c-Myc expression, and induces apoptosis in HCT-116 cells. These findings suggest that the inhibition of CDK7 may be a viable approach to suppress Myc expression.

Oral administration of UD-017 inhibited tumor growth in the HCT-116 xenograft mouse model in a dose-dependent manner. According to one *in vitro* study, the activation of p53 by 5-FU synergized with a CDK7 inhibitor to induce cell death<sup>14</sup>). Another *in vitro* study reported that a CDK4/6 inhibitor showed synergistic effects on cancer cells when combined with 5-FU by modulating thymidylate synthase expression<sup>21</sup>). However, to our knowledge, there are no reports of highly selective CDK7 inhibitors showing synergistic effects with 5-FU in *in vivo* models. In this study, we demonstrated the synergistic effects of UD-017 in combination with 5-FU in the HCT-116 xenograft mouse model. Co-administration of UD-017 and 5-FU may induce apoptosis more strongly through p53 activation and affect the expression of thymidylate synthase, although this will need to be evaluated in future studies.

In conclusion, the highly selective CDK7 inhibitor, UD-017, significantly inhibited the proliferation of a human colorectal cancer cell line (HCT-116) by inducing cell-cycle arrest and apoptosis, and by regulating gene expression, both *in vitro* and *in vivo* (Figure 7). We anticipate that UD-017 will show anticancer effects in clinical trials through this mechanism.

## **ACKNOWLEDGMENTS**

We thank our colleagues for their generous support.

## REFERENCES

- 1 Akhtar, M. S., Heidemann, M., Tietjen, J. R., Zhang, D. W., Chapman, R. D., Eick, D., et al. 2009. TFIIF kinase places bivalent marks on the carboxy-terminal domain of RNA polymerase II. *Molecular Cell*. 34:387–393.
- 2 Ali, S., Heathcote, D. A., Kroll, S. H., Jogalekar, A. S., Scheiper, B., Patel, H., et al. 2009. The development of a selective cyclin-dependent kinase inhibitor that shows antitumor activity. *Cancer Research*. 69:6208–6215.
- 3 Beaver, J. A., Amiri-Kordestani, L., Charlab, R., Chen, W., Palmby, T., Tilley, A., et al. 2015. FDA Approval: Palbociclib for the treatment of postmenopausal patients with estrogen receptor-positive, HER2-negative metastatic breast cancer. *Clinical Cancer Research*. 21:4760–4766.
- 4 Bhullar, K. S., Lagarón, N. O., McGowan, E. M., Parmar, I., Jha, A., Hubbard, B. P., et al. 2018. Kinase-targeted cancer therapies: progress, challenges and future directions. *Molecular Cancer*. 17:48.
- 5 Boeing, S., Rigault, C., Heidemann, M., Eick, D. and Meisterernst, M. 2010. RNA polymerase II C-terminal heptarepeat domain Ser-7 phosphorylation is established in a mediator-dependent fashion. *The Journal of biological chemistry*. 285:188–196.
- 6 Chen, B. J., Wu, Y. L., Tanaka, Y. and Zhang, W. 2014. Small molecules targeting c-Myc

- oncogene: promising anti-cancer therapeutics. *International Journal of Biological Sciences*. 10:1084–1096.
- 7 Chipumuro, E., Marco, E., Christensen, C. L., Kwiatkowski, N., Zhang T., Hatheway, C. M., et al. 2014. CDK7 inhibition suppresses super-enhancer-linked oncogenic transcription in MYCN-driven cancer. *Cell* 159:1126–1139.
  - 8 Christensen, C. L., Kwiatkowski, N., Abraham, B. J., Carretero, J., Al-Shahrour, F., Zhang, T., et al. 2014. Targeting transcriptional addictions in small cell lung cancer with a covalent CDK7 inhibitor. *Cancer Cell*. 26:909–922.
  - 9 Dickler, M. N., Tolaney, S. M., Rugo, H. S., Cortés, J., Diéras, V., Patt, D., et al. 2017. MONARCH 1, A phase II study of Abemaciclib, a CDK4 and CDK6 inhibitor, as a single agent, in patients with refractory HR+/HER2- metastatic breast cancer. *Clinical Cancer Research*. 23:5218–5224.
  - 10 Fisher, R. P. and Morgan, D. O. 1994. A novel cyclin associates with M015/CDK7 to form the CDK-activating kinase. *Cell* 78:713–724.
  - 11 Glover-Cutter, K., Larochele, S., Erickson, B., Zhang, C., Shokat, K., Fisher, R. P., et al. 2009. TFIIF-associated Cdk7 kinase functions in phosphorylation of C-terminal domain Ser7 residues, promoter-proximal pausing, and termination by RNA polymerase II. *Molecular and Cellular Biology*. 29: 5455–5564.

- 12 Hnisz, D., Abraham, B. J., Lee, T. I., Lau, A., Saint-André, V., Sigova, A. A., et al. 2013.  
Super-enhancers in the control of cell identity and disease. *Cell*. 155:934–947.
- 13 Hu, S., Marineau, J. J., Rajagopal, N., Hamman, K. B., Choi, Y. J., Schmidt, DR., et al.  
2019. Discovery and Characterization of SY-1365, a Selective, Covalent Inhibitor of CDK7.  
*Cancer Research* 79:3479–3491.
- 14 Kalan, S., Amat, R., Schachter, M.M., Kwiatkowski, N., Abraham, B.J., Liang, Y., et al.  
2017. Activation of the p53 Transcriptional Program Sensitizes Cancer Cells to Cdk7  
Inhibitors. *Cell Report*. 21:467-481.
- 15 Kelso, T.W., Baumgart, K., Eickhoff, J., Albert, T., Antrecht, C., Lemcke, S., et al. 2014.  
Cyclin-dependent kinase 7 controls mRNA synthesis by affecting stability of preinitiation  
complexes, leading to altered gene expression, cell cycle progression, and survival of tumor  
cells. *Molecular and Cellular Biology*. 34:3675-3688.
- 16 Komarnitsky, P., Cho, E. J. and Buratowski, S. 2000. Different phosphorylated forms of  
RNA polymerase II and associated mRNA processing factors during transcription. *Genes &  
Development*. 14:2452–2460.
- 17 Kwiatkowski, N., Zhang, T., Rahl, P. B., Abraham, B. J., Reddy, J., Ficarro, S. B., et al.  
2014. Targeting transcription regulation in cancer with a covalent CDK7 inhibitor. *Nature*.  
511:616–620.

- 18 Lovén, J., Hoke, H. A., Lin, C. Y., Lau, A., Orlando, D. A., Vakoc, C.R., et al. 2013. Selective inhibition of tumor oncogenes by disruption of super-enhancers. *Cell*. 153:320–334.
- 19 Malumbres, M. 2014. Cyclin-dependent kinases. *Genome Biology*. 15:122–131.
- 20 Mansour, M. R., Abraham, B. J., Anders, L., Berezovskaya, A., Gutierrez, A., Durbin, A. D., et al. 2014. Oncogene regulation. An oncogenic super-enhancer formed through somatic mutation of a noncoding intergenic element. *Science* 346:1373–1377.
- 21 Min, A., Kim, J.E., Kim, Y.J., Lim, J.M., Kim, S., Kim, J.W., et al. 2018. Cyclin E overexpression confers resistance to the CDK4/6 specific inhibitor palbociclib in gastric cancer cells. *Cancer Letters*. 430:123-132
- 22 Pandey, K., An, H.J., Kim, S.K., Lee, S.A., Kim, S., Lim, S.M., et al. 2019. Molecular mechanisms of resistance to CDK4/6 inhibitors in breast cancer: A review. *International Journal of Cancer*. 145:1179-1188.
- 23 Patel, H., Abduljabbar, R., Lai, C. F., Periyasamy, M., Harrod, A., Gemma, C., et al. 2016. Expression of CDK7, cyclin H, and MAT1 is elevated in breast cancer and is prognostic in estrogen receptor-positive breast cancer. *Clinical Cancer Research*. 22:5929–5938.
- 24 Patel, H., Periyasamy, M., Sava, G. P, Bondke, A., Slafer, B. W., Kroll, S. H. B., et al. 2018. ICEC0942, an Orally Bioavailable Selective Inhibitor of CDK7 for Cancer Treatment.

- Molecular Cancer Therapeutics. 17:1156–1166.
- 25 Schachter, M. M., Merrick, K. A., Larochelle, S., Hirschi, A., Zhang, C., Shokat, K. M., et al. 2013. A Cdk7-Cdk4 T-Loop Phosphorylation Cascade Promotes G1 Progression. *Molecular Cell*. 50:250–260.
  - 26 Tripathy, D., Bardia, A. and Sellers, W. R. 2017. Ribociclib (LEE011): Mechanism of action and clinical impact of this selective cyclin-dependent kinase 4/6 inhibitor in various solid tumors. *Clinical Cancer Research*. 23:3251–3262.
  - 27 Wang, B. Y., Liu, Q. Y., Cao, J., Chen, J. W. and Liu, Z. S. 2016. Selective CDK7 inhibition with BS-181 suppresses cell proliferation and induces cell cycle arrest and apoptosis in gastric cancer. *Drug Design, Development and Therapy*. 10:1181–1189.
  - 28 Wang, Q., Li, M., Zhang, X., Huang, H., Huang, J., Ke, J., et al. 2016. Upregulation of CDK7 in gastric cancer cell promotes tumor cell proliferation and predicts poor prognosis. *Experimental and Molecular Pathology*. 100: 514–521.
  - 29 Wang, X. N., Su, X. X., Cheng, S. Q., Sun, Z. Y., Huang, Z. S and Ou, T. M. 2019. MYC modulators in cancer: a patent review. *Expert Opinion on Therapeutic Patents*. 29:353–367.
  - 30 Wiernik P. H. 2016. Alvocidib (flavopiridol) for the treatment of chronic lymphocytic leukemia. *Expert Opinion on Investigational Drugs*. 25:729–734.
  - 31 Zhang, J., Yang, X., Wang, Y., Shi, H., Guan, C., Yao, L., et al. 2013. Low expression of

- cyclinH and cyclin-dependent kinase 7 can decrease the proliferation of human esophageal squamous cell carcinoma. *Digestive Diseases and Sciences*. 58:2028–2037.
- 32 Zhang, Y.X., Sicinska, E., Czaplinski, J.T., Remillard, S.P., Moss, S., Wang, Y., et al. 2014. Antiproliferative effects of CDK4/6 inhibition in CDK4-amplified human liposarcoma in vitro and in vivo. *Molecular Cancer Therapeutics*. 13:2184-2193.
- 33 Zhang, Z., Peng, H., Wang, X., Yin, X., Ma, P., Jing, Y., et al. 2017. Preclinical Efficacy and Molecular Mechanism of Targeting CDK7-Dependent Transcriptional Addiction in Ovarian Cancer. *Molecular Cancer Therapeutics*. 16:1739–1750.
- 34 Zhou, Y., Lu, L., Jiang, G., Chen, Z., Li, J., An, P., et al. 2019. Targeting CDK7 increases the stability of Snail to promote the dissemination of colorectal cancer. *Cell Death & Differentiation*. 26:1442-1452.

## FIGURE and TABLE LEGENDS

Figure 1. *In vitro* properties of UD-017 as a CDK7 inhibitor.

(A) UD-017 selectivity for various kinases. Specificity of UD-017 (1000 nM) was tested against a panel of 313 kinases. IC<sub>50</sub> values were calculated for kinases that showed more than 50% inhibition at 1000 nM of UD-017. (B) Selectivity of UD-017 for various CDK subtypes. (C) GI<sub>50</sub> values of UD-017 against colorectal cancer cell lines.

Figure 2. Mechanism underlying the antiproliferative effects of UD-017 in HCT-116 cells.

(A) Effect of UD-017 on the phosphorylation of CDKs and Rb protein in HCT-116 cells at 8 and 24 hrs after treatment. CDK1, pCDK1, CDK2, pCDK2: 34 kDa. Rb, pRb: 110kDa. GAPDH: 37kDa. (B) Effect of UD-017 on cell cycle progression in HCT-116 cells at 8 hrs after treatment (n = 2). Band densities were quantified and normalized to DMSO control.

Figure 3. Induction of apoptosis by UD-017 in HCT-116 cells.

(A) Effect of UD-017 on phosphorylation of RNAPII in HCT-116 cells at 1 to 72 hrs after treatment. RNAPII, pRNAPII: 240 kDa. (B) Effect of UD-017 on Myc expression in HCT-116 cells at 1 to 72 hrs after treatment. c-Myc: 57-65 kDa. (C) Expression of apoptosis-related proteins at 72 hrs after

treatment with UD-017 in HCT-116 cells. XIAP: 53 kDa, PARP: 116 kDa, cleaved PARP: 89 kDa.

(D) Apoptosis induction in HCT-116 cells at 72 hrs after treatment with UD-017 (n = 3–6). Band densities were quantified and normalized to DMSO control. Data are presented as mean  $\pm$  SD.

Dunnett's multiple test using EXSUS, \*\*\*:  $P < 0.001$ .

Figure 4. Anticancer activity of UD-017 in HCT-116 xenograft mouse model.

(A) *In vivo* anticancer activity of UD-017 after 14 days of treatment. (B) Body weight change after UD-017 treatment. Data are presented as mean  $\pm$  SE (n = 6). Dunnett's multiple test using EXSUS,

\* $p < 0.05$ , \*\* $p < 0.01$ , \*\*\* $p < 0.001$  versus vehicle group.

Figure 5. Mechanism underlying anticancer activity of UD-017 in HCT-116 xenograft mouse model.

(A) Phosphorylation of Rb protein at 2 hrs after administration of a single dose of UD-017 (100

mg/kg). Rb, pRb: 110kDa. NC: not calculated. (B) Phosphorylation of RNAPII protein, expression

of c-Myc, and PARP cleavage at 2 hrs after administration of a daily single dose of UD-017 (25, 50,

100 mg/kg). RNAPII, pRNAPII: 240kDa. c-Myc: 57-65kDa. PARP: 116kDa, cleaved PARP: 89kDa.

Band densities were quantified and ratios were calculated.

Figure 6. Combination treatment of HCT-116 xenograft mouse model with UD-017 and 5-FU.

(A) *In vivo* anticancer activity of UD-017 with 5-FU after 14 days of treatment. (B) Body weight change after UD-017 with 5-FU treatment. Data are presented as mean  $\pm$  SE (n = 6). Dunnett's multiple test using EXSUS, \*p < 0.05, UD-017 50 mg/kg + 5-FU 15 mg/kg group versus UD-017 50 mg/kg group.

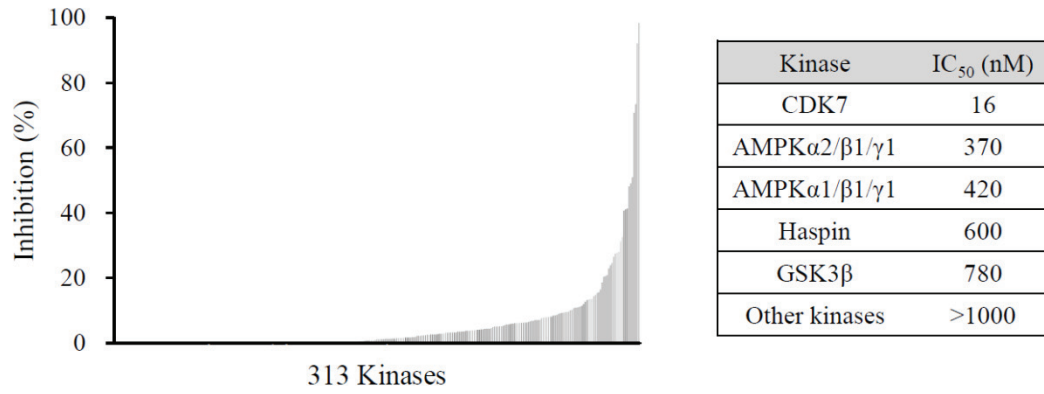
Figure 7. Schematic of proposed mechanism of action of UD-017 in HCT-116 cells.

UD-017 suppresses phosphorylation of CDK1, 2, and 4/6, which is followed by cell cycle arrest.

UD-017 also prevents phosphorylation of RNAPII and reduces the transcription of c-Myc, which plays an important role in cell survival. Apoptosis is induced by the activation of apoptosis-related proteins.

Figure 1

(A)



(B)

CDK subtypes	IC <sub>50</sub> (nM)
CDK1 (CycB1)	>10,000
CDK2 (CycA2)	6200
CDK2 (CycE1)	8900
CDK3 (CycE1)	>10,000
CDK4 (CycD3)	>10,000
CDK5 (p25)	5100
CDK6 (CycD3)	>10,000
CDK7 (CycH/MAT1)	16
CDK9 (CycT1)	>10,000

(C)

Cell line	GI <sub>50</sub> (nM)
HCT-116	19
Lovo	110
LS-174T	80
SW48	80
SW620	120

Figure 2

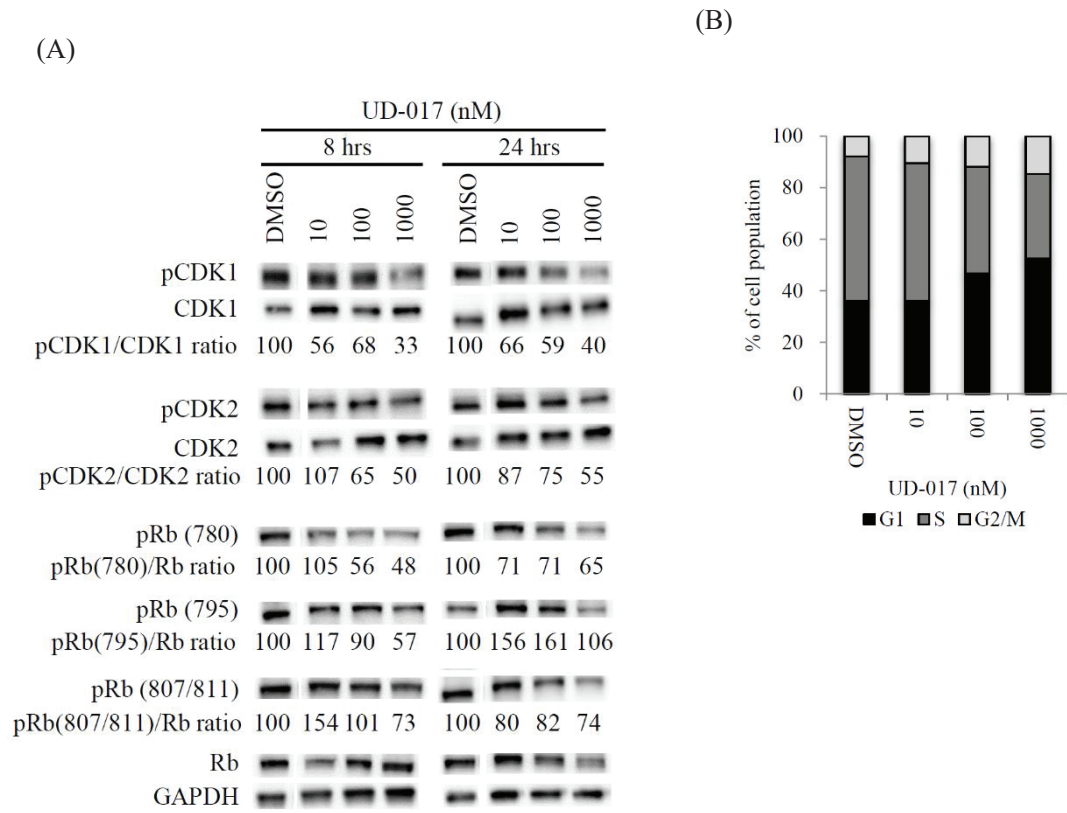
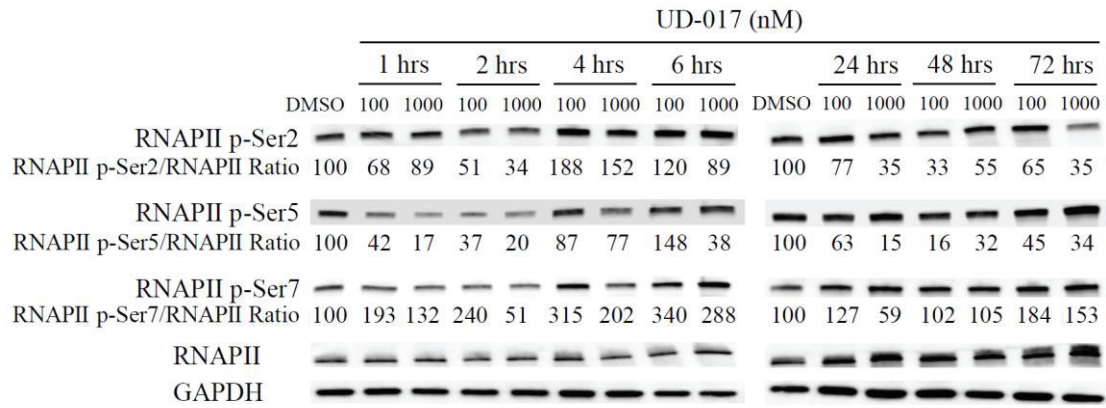
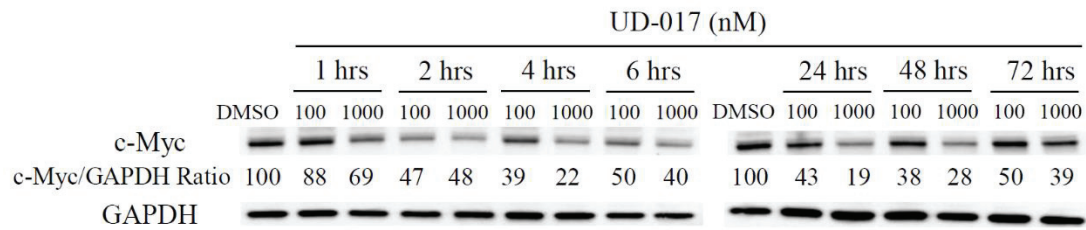


Figure 3

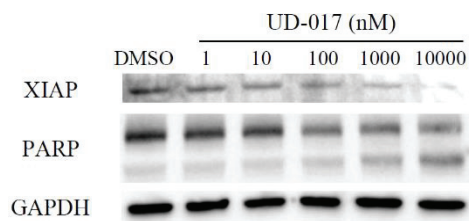
(A)



(B)



(C)



(D)

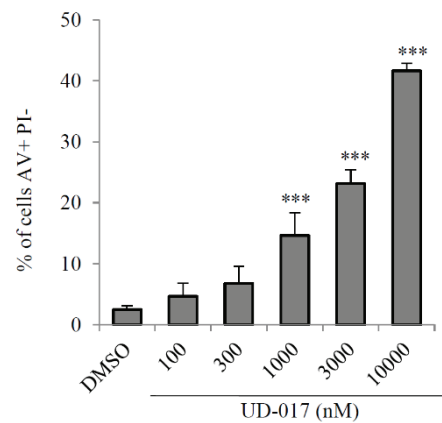
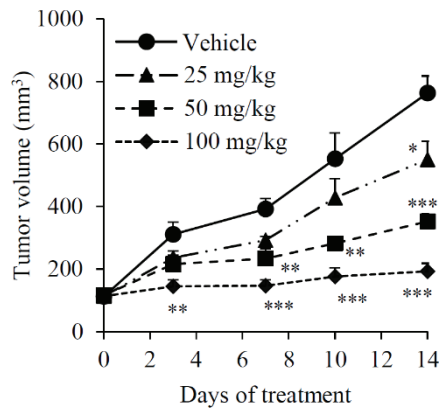


Figure 4

(A)



(B)

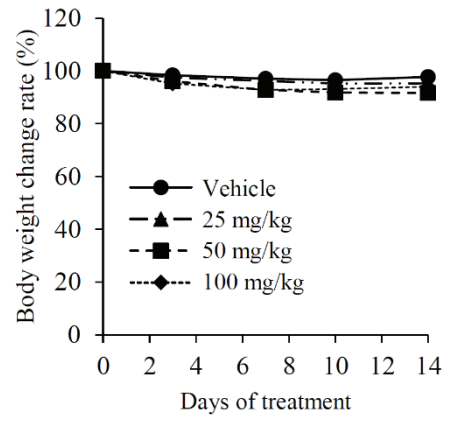
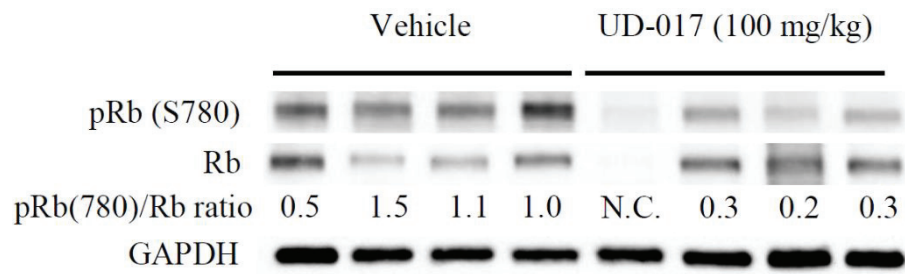


Figure 5

(A)



(B)

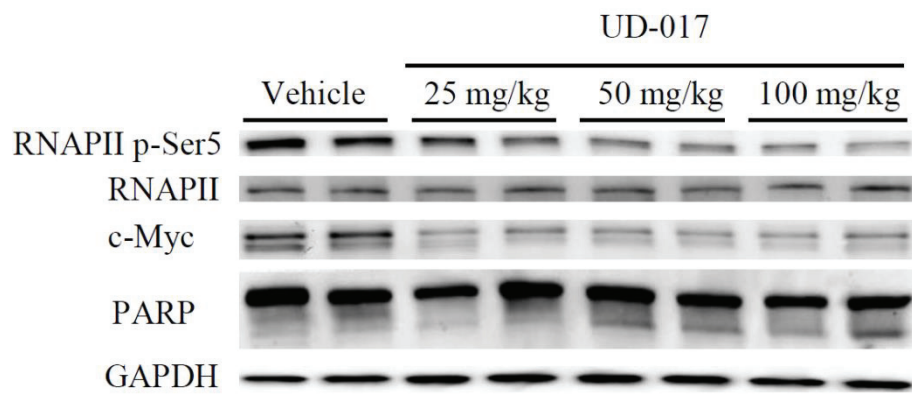
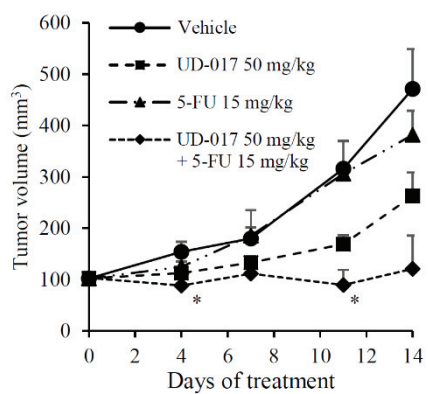


Figure 6

(A)



(B)

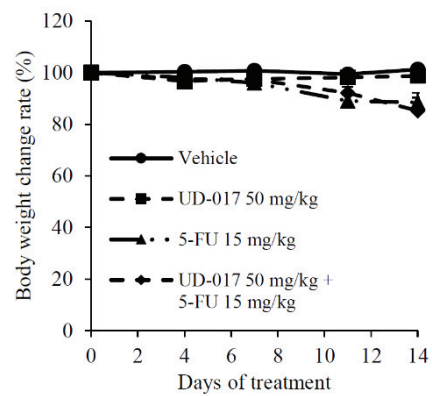


Figure 7

